Electronic Supplementary Information for:

Exchange Coupling and Single Molecule Magnetism in Redox-active Tetraoxolene-bridged Dilanthanide Complexes

Peng Zhang,[a] Mauro Perfetti,[a,b] Michal Kern,[a] Philipp P. Hallmen,[a] Liviu Ungur,[c] Samuel Lenz,[a] Mark R. Ringenberg,[d] Wolfgang Frey,[e] Hermann Stoll,[f] Guntram Rauhut,[f] Joris van Slageren*,[a]

[a] Institut für Physikalische Chemie, Universität Stuttgart, Pfaffenwaldring 55, D-70569, Stuttgart, Germany

[b] Department of Chemistry, University of Copenhagen, Universitetparken 5, 2100 Copenhagen, Denmark

[c] Theory of Nanomaterials Group and INPAC-Institute of Nanoscale Physics and Chemistry, Katholieke, Universiteit Leuven, 3001 Leuven, Belgium

[d] Institut für Anorganische Chemie, Universität Stuttgart, Pfaffenwaldring 55, D-70569 Stuttgart, Germany

[e] Institut für Organische Chemie, Universität Stuttgart, Pfaffenwaldring 55, D-70569 Stuttgart, Germany

[f] Institut für Theoretische Chemie, Universität Stuttgart, Pfaffenwaldring 55, D-70569 Stuttgart, Germany

Table of Contents

***Ab initio* calculations**

Multi-configurational *ab initio* calculations were performed for **1Tb** and **1Dy**, replacing one of the two Tb^{3+}/ Dy^{3+} by diamagnetic Y^{3+}. The calculations were carried out with the Molpro[1,2] suite of *ab initio* programs using the measured crystal structure. The (state-averaged) orbitals were obtained by employing the local density-fitted configuration-averaged Hartree-Fock (LDF-CAHF) method[3,4]. The active space included 8 electrons of Tb^{III}/9 electrons of Dy^{III} in seven 4f-type orbitals. The 28 electron pseudopotential/effective core potential (ECP) ECP28MWB[5,6] was used for Tb/Dy and Y. The basis set employed for Tb/Dy and Y was def2-TZVPP[7] and the auxiliary basis set for density fitting def2-TZVPP-JKFIT[7]. The elements O and N were described by the cc-pVTZ[8–10] basis set and the corresponding auxiliary basis set for these elements was cc-pVTZ-JKFIT[11]. For the remaining elements except of H, the cc-pVDZ[8–10] basis set and the corresponding cc-pVDZ-JKFIT[11] basis set for density fitting were used. The hydrogen atoms were described by a minimal basis (MINAO)[12] and the auxiliary basis set cc-pVDZ-JKFIT[11] was employed for density fitting. In the spin-orbit coupling step the ECP-SO operator corresponding to ECP28MWB was employed[5]. The orbitals resulting from the LDF-CAHF calculation are equivalent to the orbitals of a state-averaged CASSCF calculation averaging over all possible roots, i.e. 7 septets, 140 quintets, 588 triplets and 490 singlets for **1Tb** and 21 sextets, 224 quartets and 490 doublets for **1Dy**, taking into account the M_S-degeneracy of the corresponding spin-manifold by a weighting factor, i.e. a weighting factor of 7 for the septets, 5 for the quintets, 3 for the triplets and 1 for the singlets (**1Tb**) and moreover 3 for the sextets, 2 for the quartets and 1 for the doublets (**1Dy**). The state-averaged orbitals were used in a subsequent CASCI (complete active space configuration interaction) step to obtain the multi-configurational spin-free wave functions. In the following SO-coupling step, a limited number of roots was mixed, i. e., all septets (7), all quintets (140), 294 triplets and 292 singlets for **1Tb** and 21 sextets, 128 quartets and 130 doublets for **1Dy**, respectively. On the basis of the resulting spin-orbit multiplets, the g_Z-value of the lowest pseudo-doublet and its direction for **1Tb** and the *g*-tensor for the ground Kramers doublet of **1Dy**, as well as the composition of the wave functions in terms of m_j-microstates for both compounds, were calculated using the SINGLE_ANISO[13] program.

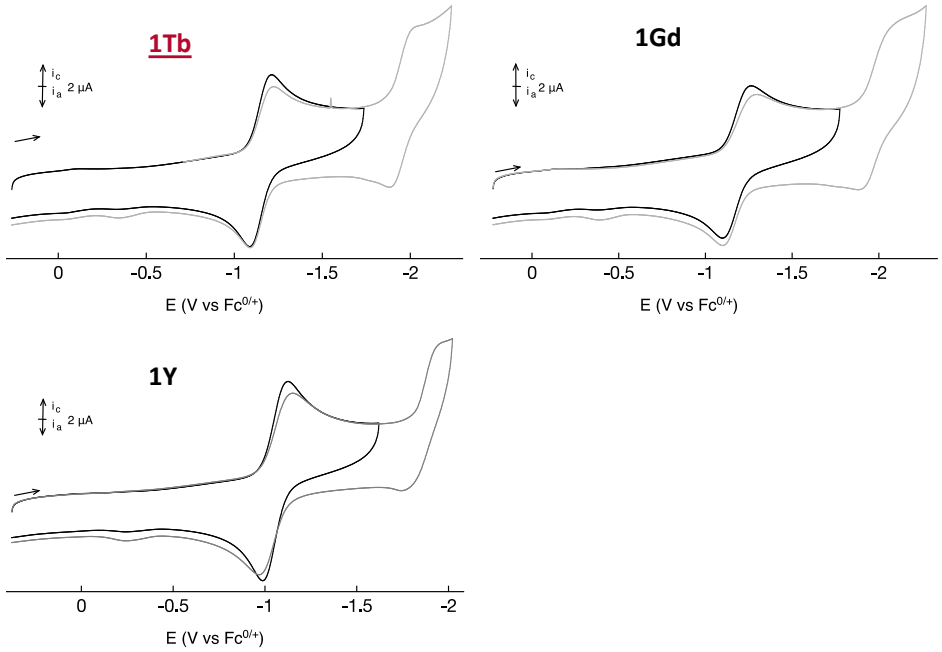

Fig. S1. Cyclic voltammogram of **1Tb**, **1Gd** and **1Y** in CH_2Cl_2/0.1 M Bu_4NPF_6 measured at 295 K. $Fc^{0/+}$ = ferrocene/ferrocenium couple.

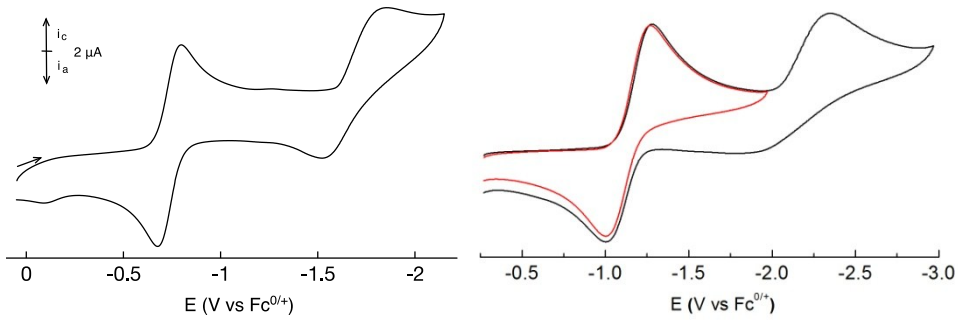

Fig. S2. Cyclic voltammogram of **1Dy** in CH_3CN (Left) and THF (Right) /0.1 M Bu_4NPF_6 measured at 295 K. $Fc^{0/+}$ = ferrocene/ferrocenium couple.

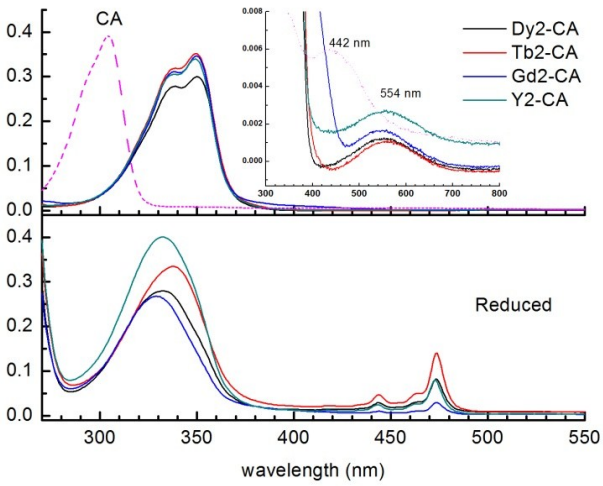

Fig. S3. UV-vis electronic absorption spectra of compound **1Ln** (top) and **2Ln** (bottom) in CH_3CN.

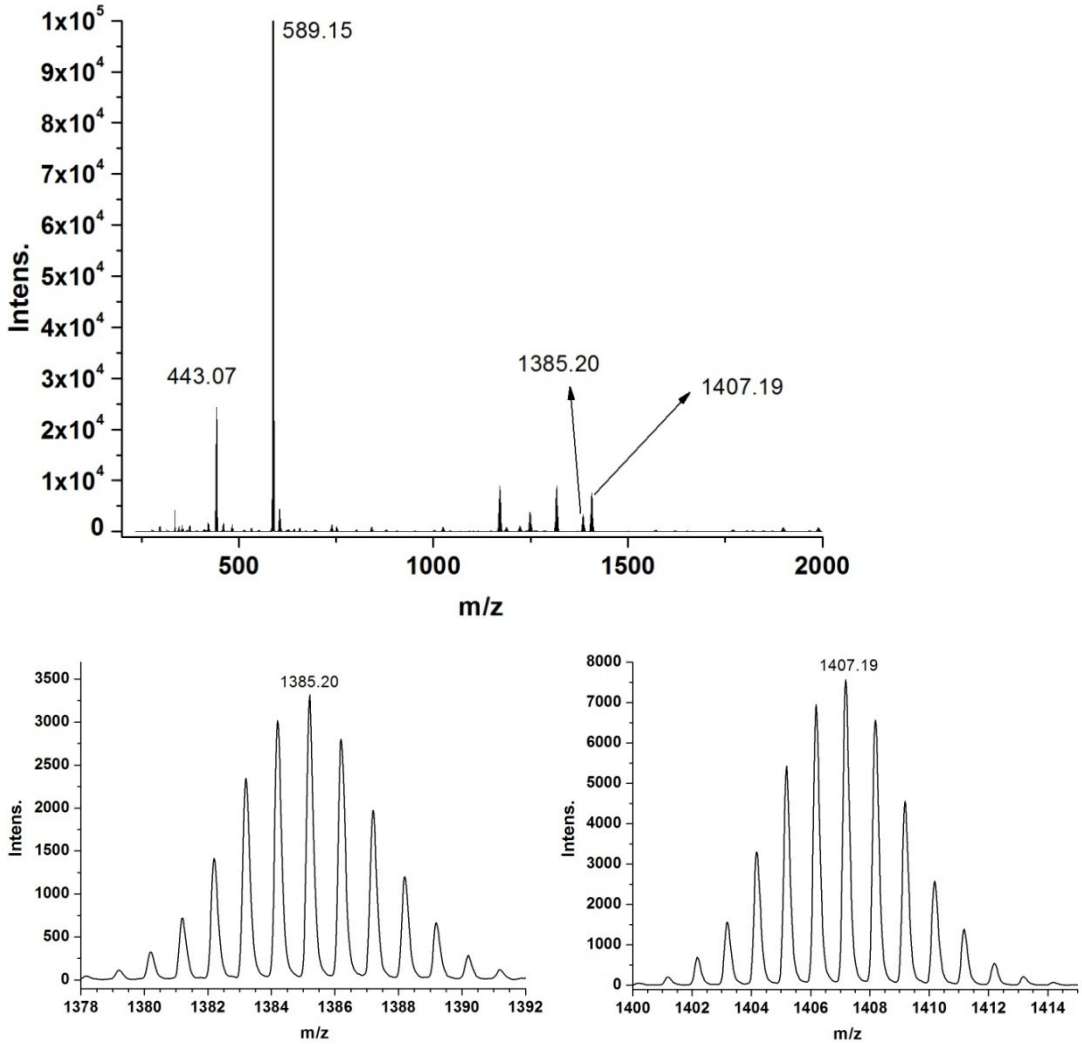

Fig. S4. ESI-MS spectra of compound **1Dy** in positive mode. m/z 1385 and 1407 correspond to $[M+H]^+$ and $[M+Na]^+$.

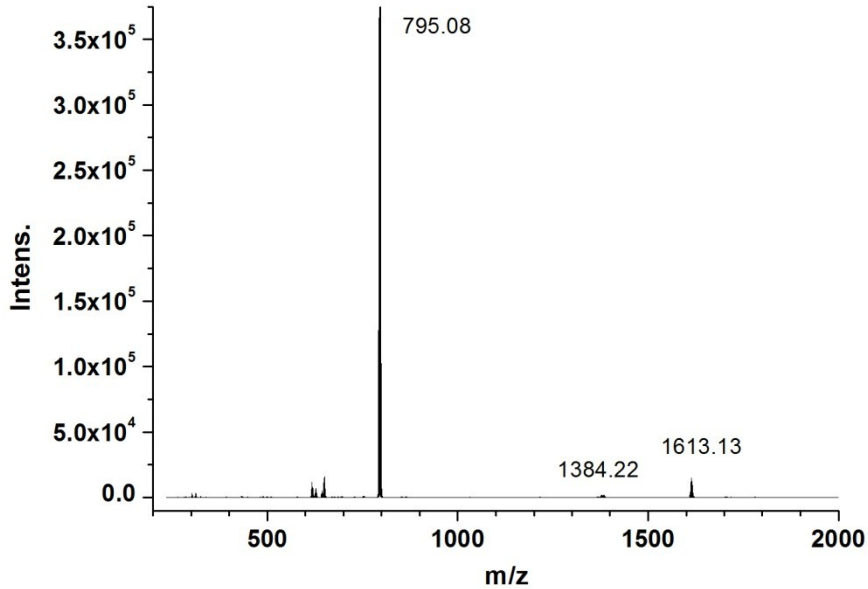

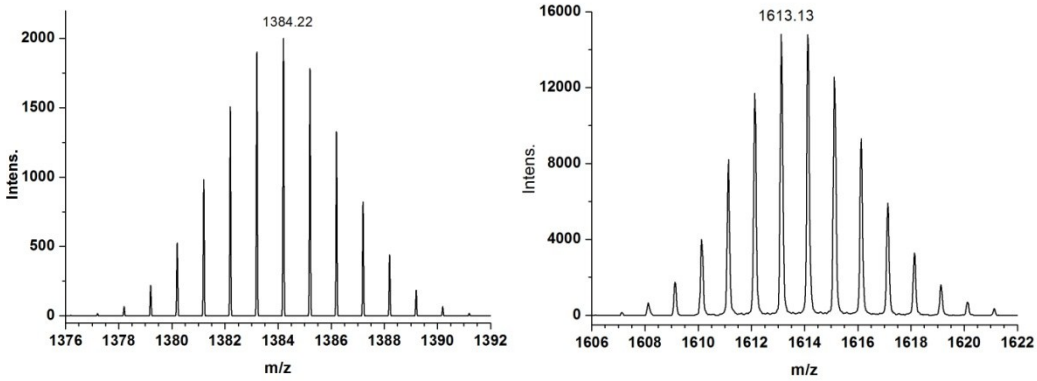

Fig. S5. ESI-MS spectra of compound **2Dy** in negative mode. m/z 1384 and 1613 correspond to $[M]^-$ and $[M+2(TFA)]^-$. TFA = Trifluoroacetic acid

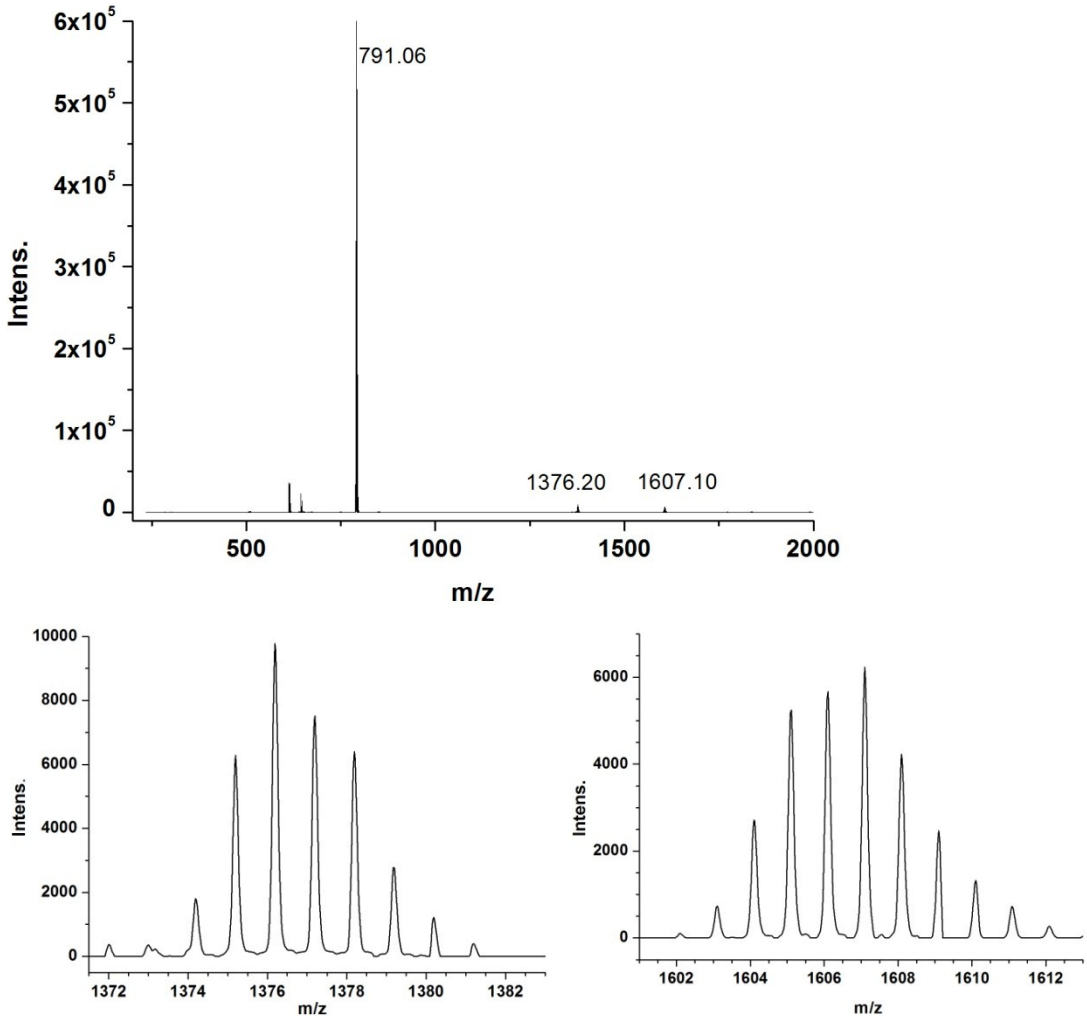

Fig. S6. ESI-MS spectra of compound **2Tb** in negative mode. m/z 1376 and 1607 correspond to $[M]^-$ and $[M+2(TFA)]^-$. TFA = Trifluoroacetic acid

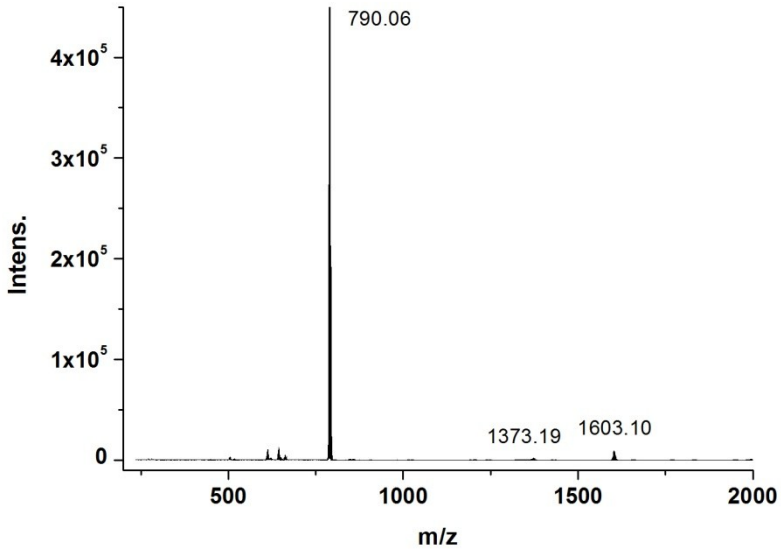

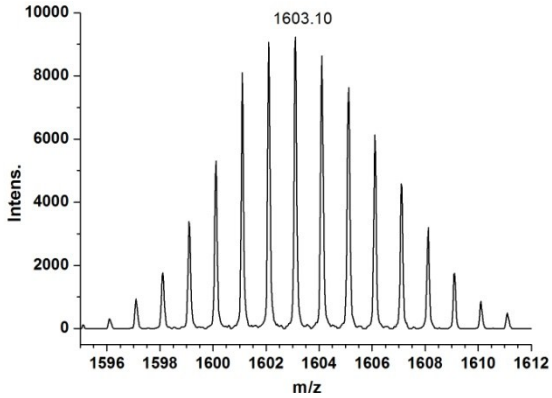

Fig. S7. ESI-MS spectra of compound **2Gd** in negative mode. m/z 1603 corresponds to [M+2(TFA)]⁻. TFA = Trifluoroacetic acid

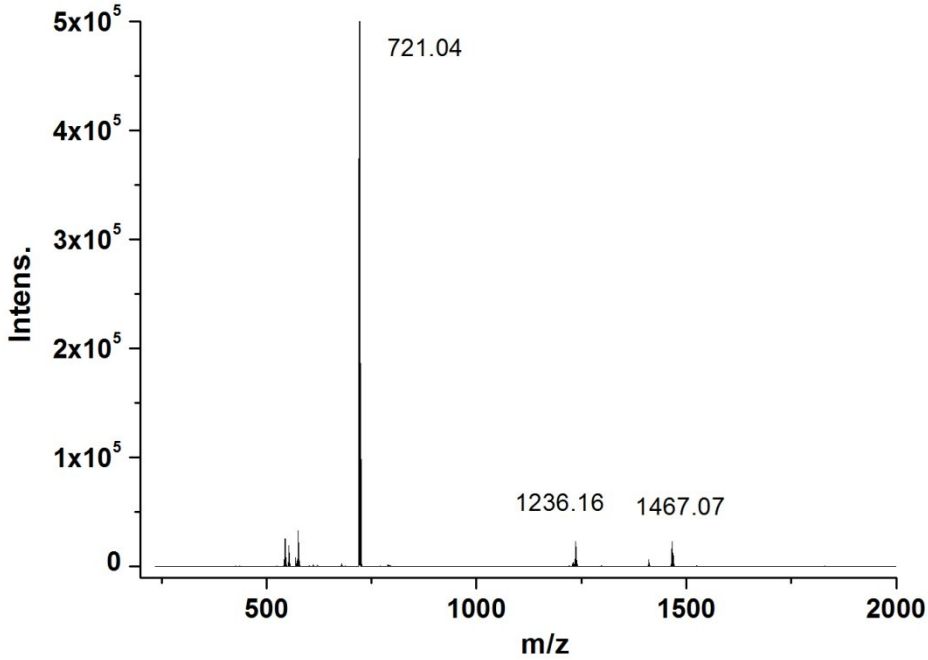

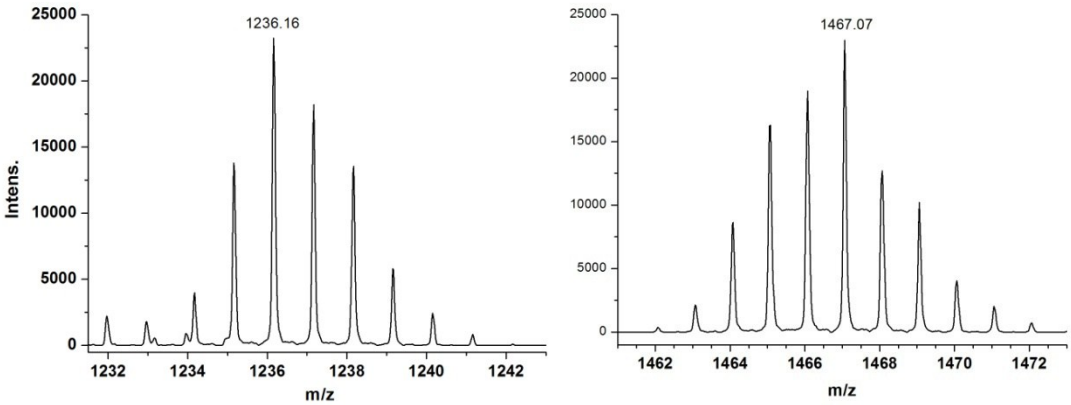

Fig. S8. ESI-MS spectra of compound **2Y** in negative mode. m/z 1236 and 1467 correspond to $[M]^-$ and $[M+2(TFA)]^-$. TFA = Trifluoroacetic acid

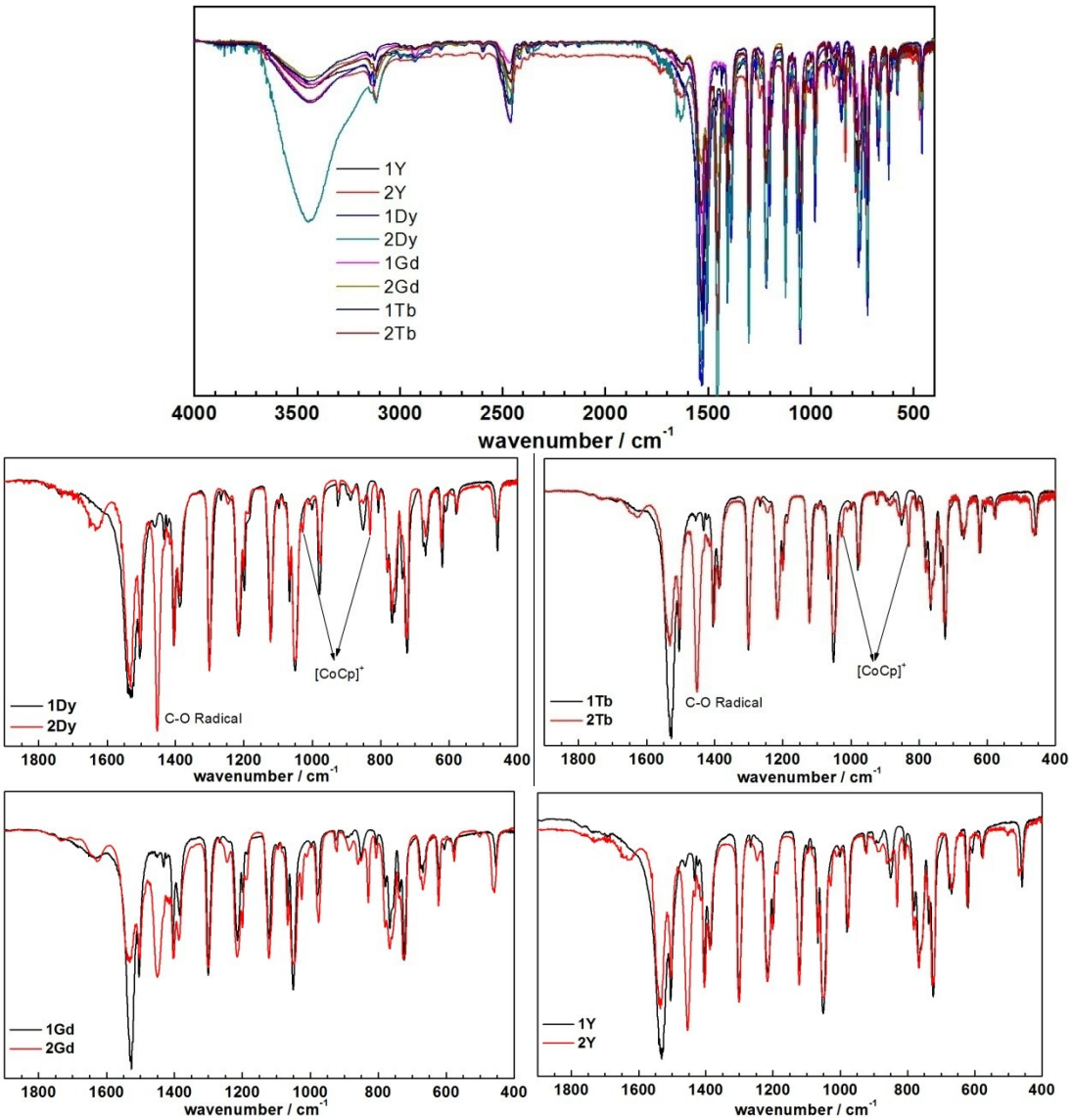

Fig. S9. IR spectra of compounds **1Ln** and **2Ln**.

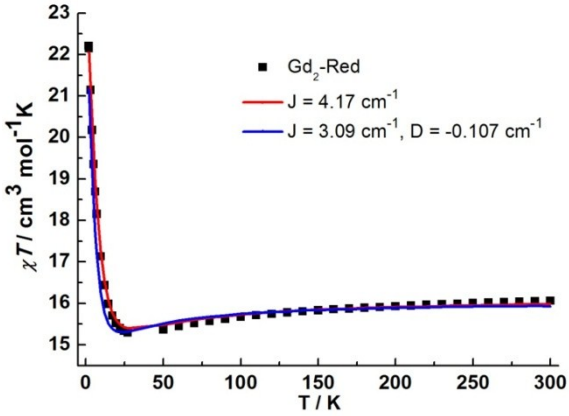

Fig. S10. The fit of $\chi_M T$ *vs* T plots for **2Gd**. The red line corresponds to the fit to a isotropic Hamiltonian only and blue line corresponds to the fit using parameters derived from HFEPR.

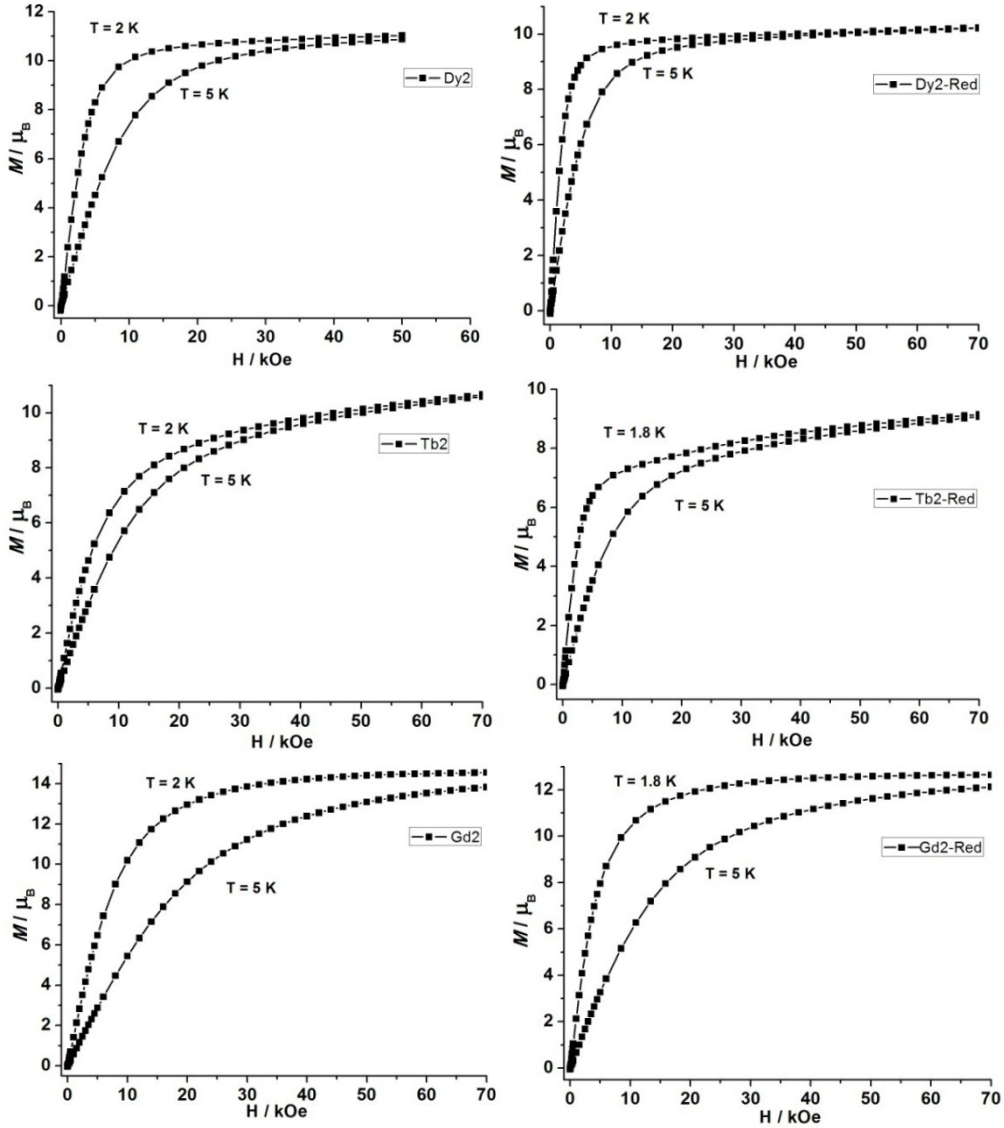

Fig. S11. Field dependences of magnetization in the field range 0-70 kOe. Left, non-radical compounds; Right, radical compounds.

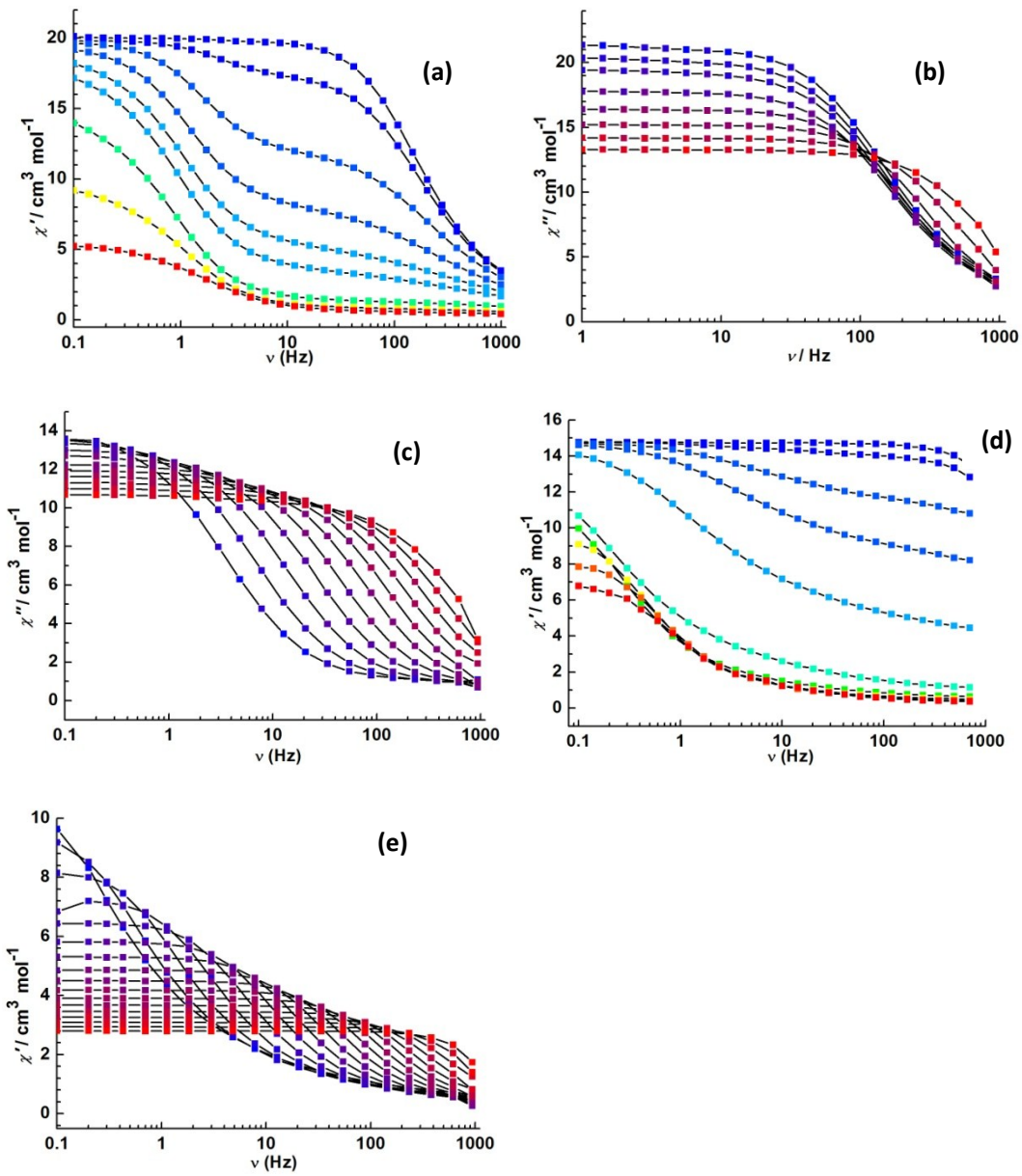

Fig. S 12. Frequency dependence of in-phase ac susceptibilities, which corresponds to Fig. 6a-e.

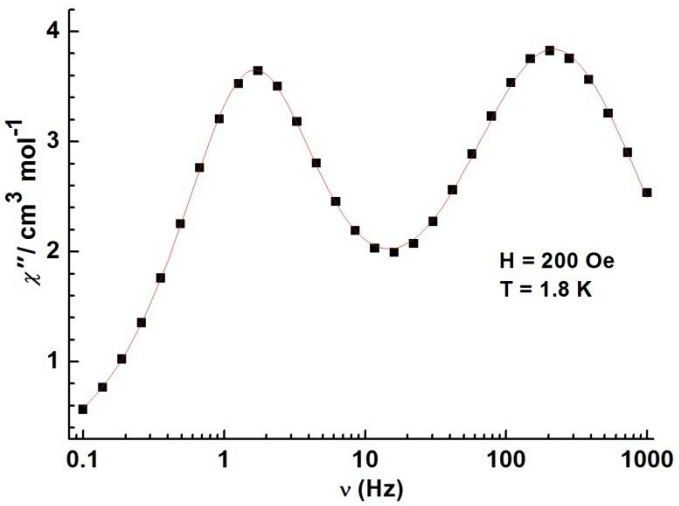

Fig. S13. An example of the least-squares-fitting (Solid line) via the sum of two modified Debye functions (200 Oe) at 1.8 K for **2Dy**.

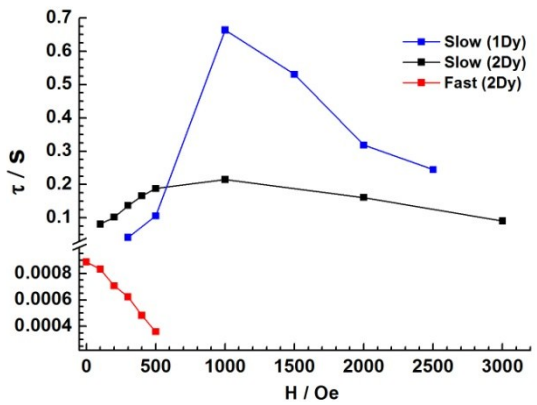

Fig. S14. Field dependence of relaxation time for compound **1Dy** and **2Dy** at 1.8 K.

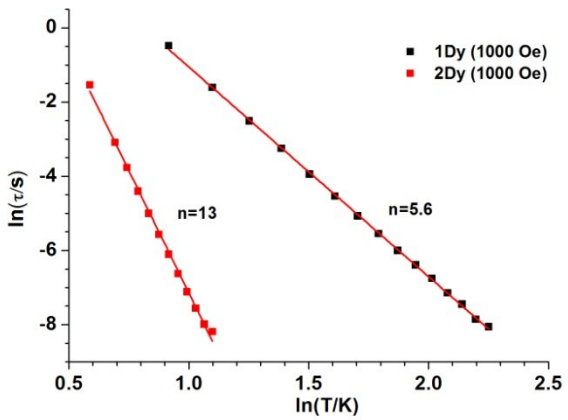

Fig. S15. ln(τ) vs ln(T) plots for compound **1Dy** and **2Dy** in 1000 Oe. The red lines correspond to the fit of $\tau^{-1} \sim T^{n}$.

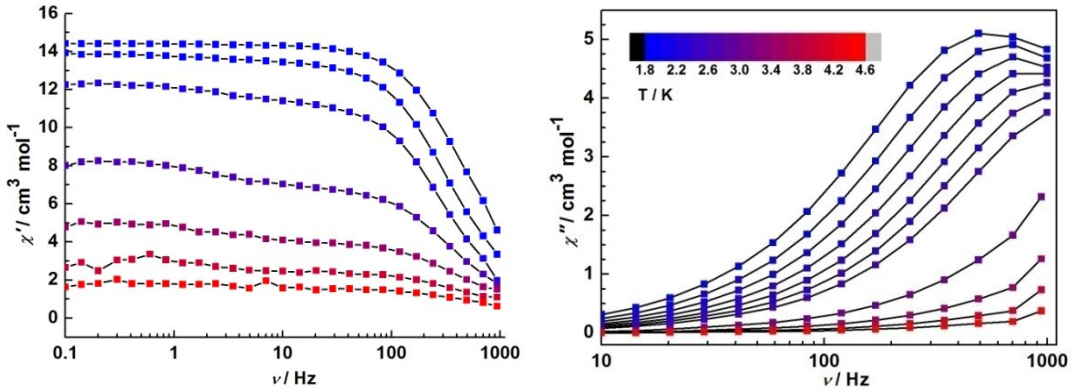

Fig. S16. Frequency and temperature dependence of ac susceptibilities under 0 Oe dc field for **2Tb**.

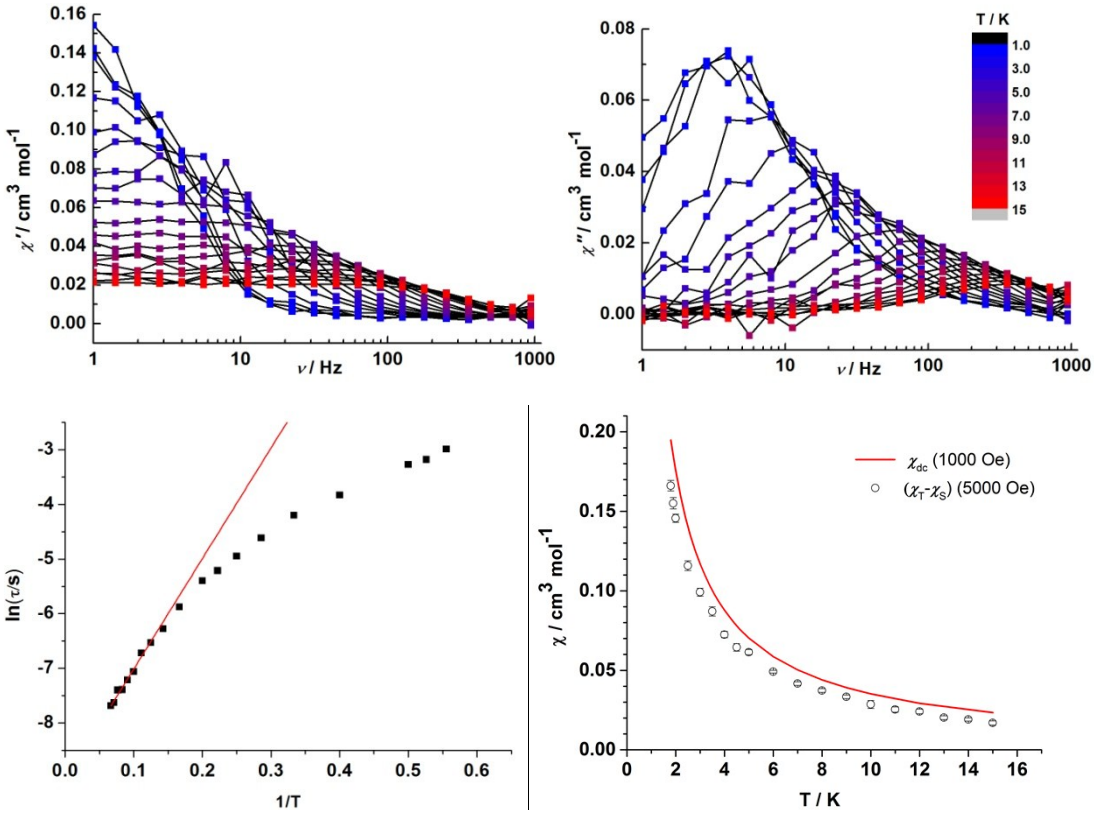

Fig. S17. Temperature dependence of ac susceptibility under 5000 Oe dc field for **2Y**, and plots of lnτ versus T^{-1} with the Arrhenius fit, and the comparison between dc susceptibility and (χ_T-χ_S) value from ac measurements.

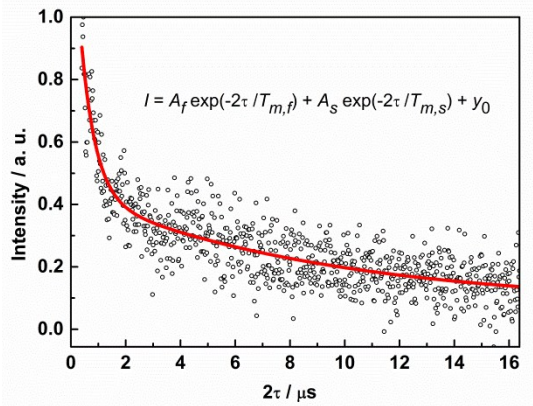

Fig. S18. Hahn-echo decay of 1mM **2Y** in acetonitrile at 7 K, 35 GHz and 1249 mT fitted with a biexponential decay function.

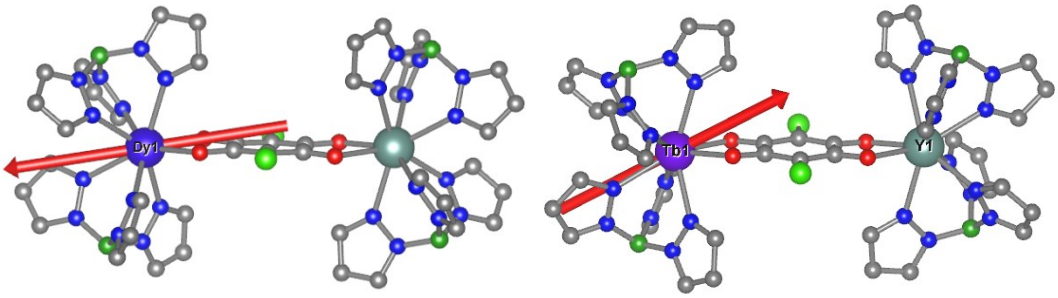

Fig. S19. The calculated orientation of the local g_z axes of ground doublets on Dy^{III} and Tb^{III} ions for **1Dy** and **1Tb**.

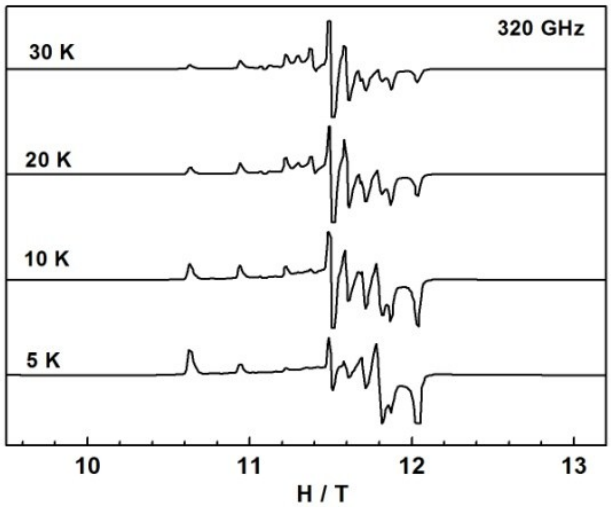

Fig. S20. HFEPR spectra of sample **Gd@1Y** recorded at 320 GHz and different temperatures.

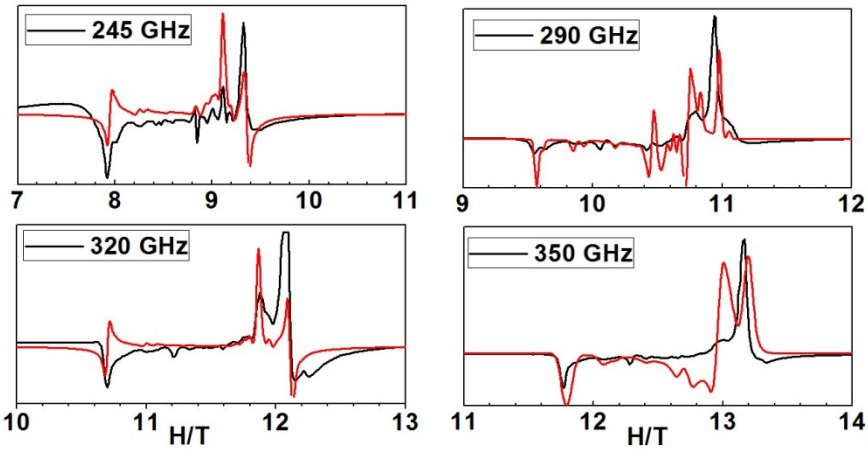

Fig. S21. HFEPR spectra of **1Gd** recorded at 5 K and various frequencies. The red lines correspond to simulations using spin Hamiltonian approach.

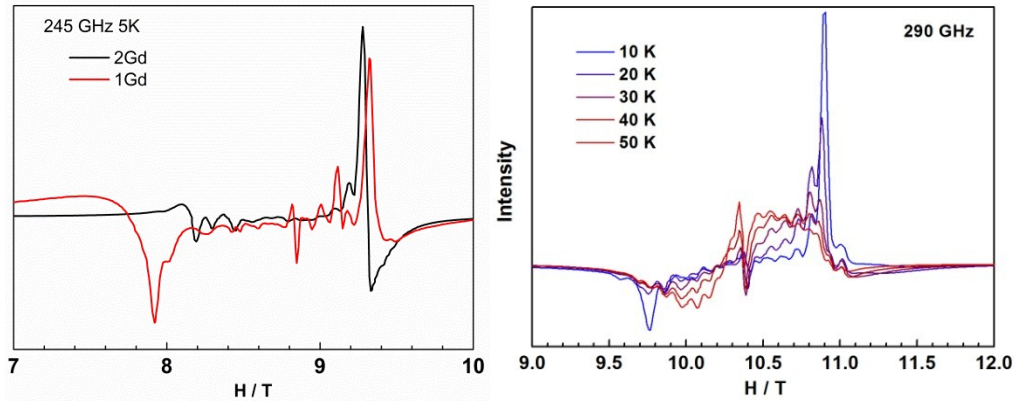

Fig. S22. The HFEPR comparison between **1Gd** and **2Gd** at 5K and 245 GHz, and spectra of sample **2Gd** recorded at 290 GHz and different temperatures.

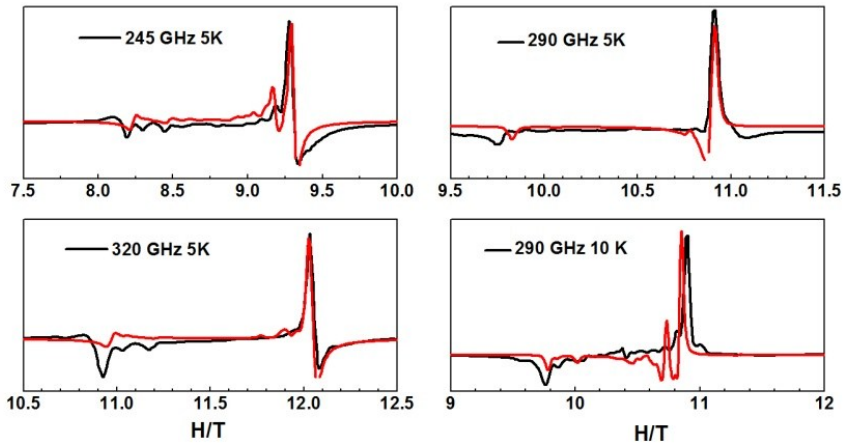

Fig. S23. HFEPR spectra of **2Gd** recorded at various frequencies. The red lines correspond to simulations using spin Hamiltonian approach.

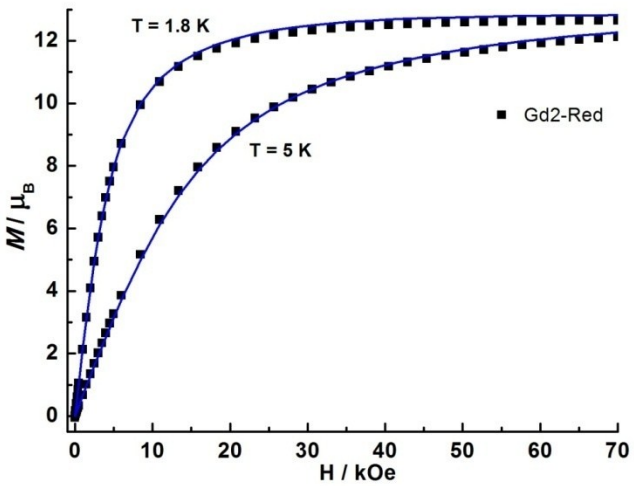

Fig. S24. The fit of magnetization for **2Gd**. The blue line corresponds to the fit using parameters derived from HFEPR parameters.

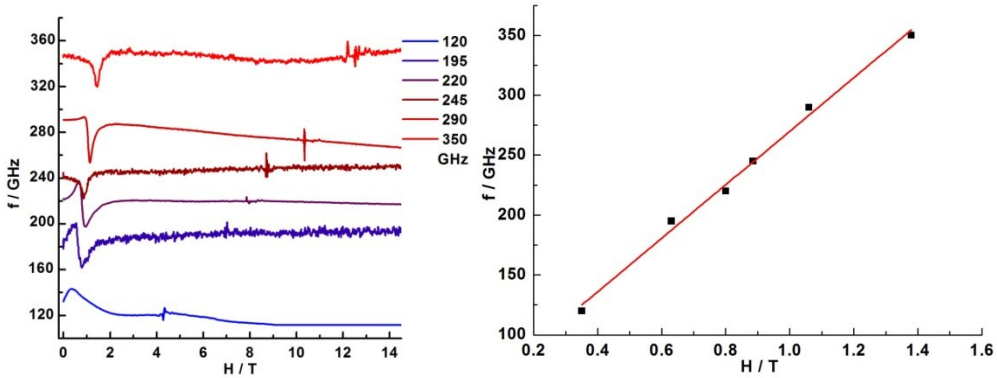

Fig. S25. HFEPR spectra of **1Tb** recorded at 5 K and various frequencies, and frequency-field plots. The red line correspond to the linear fit.

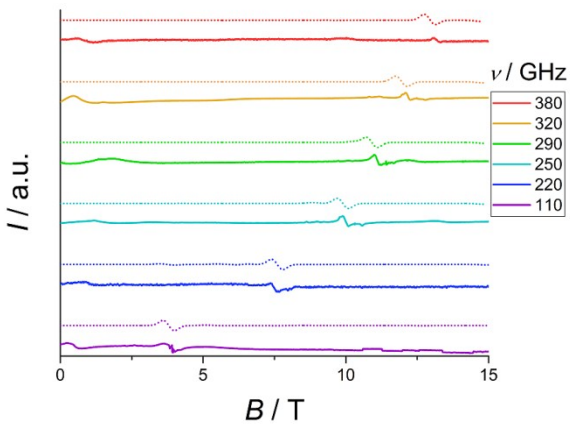

Fig. S26. Simulations of the HFEPR spectra of **2Tb**, using a model consisting of two effective spins S = 1 with D values, isotropically exchange coupled to an S = 1/2 radical. H = $J\hat{\mathbf{S}}_{\mathbf{rad}}(\hat{\mathbf{S}}_1+\hat{\mathbf{S}}_2) + \mu_B\hat{\mathbf{S}}\cdot\mathbf{g}\cdot\hat{\mathbf{H}} + \sum D\hat{S}_z^2$, with S_{rad} = 1/2, S_1 = S_2 = 1, D = –2000 cm^{-1}, E = 1 cm^{-1}, g_{rad} =2.07, g_{Tb} = (0.1, 0.1, 4.0), J = 4.3 cm^{-1}.

Table S1. Crystallographic data and structure refinement details for compounds **1Ln**

Compound	**1Dy**	**1Tb**	**1Gd**	**1Y**
Formula	$Dy_2C_{44}N_{24}O_4B_4Cl_6H_{44}$	$Tb_2C_{44}N_{24}O_4B_4Cl_6H_{44}$	$Gd_2C_{44}N_{24}O_4B_4Cl_6H_{44}$	$Y_2C_{44}N_{24}O_4B_4Cl_6H_{44}$
Mr	1553.93	1546.79	1543.44	1406.75
Crystal system	Monoclinic	Monoclinic	Monoclinic	Monoclinic
Space group	$P2_1/n$	$P2_1/n$	$P2_1/n$	$P2_1/n$
T [K]	156(2)	156(2)	296(2)	156(2)
a [Å]	13.9322	14.0030	14.1500	13.9374
b [Å]	15.0142	15.0792	15.2250	15.0463
c [Å]	14.8268	14.8247	14.9690	14.7862
α [°]	90.000	90.000	90.000	90.000
β [°]	107.692	107.593	107.750	107.464
γ [°]	90.000	90.000	90.000	90.000
V [Å^3]	2954.79	2983.88	3071.31	2957.83
Z	2	2	2	2
ρ_{calcd} [g cm^{-3}]	1.747	1.722	1.669	1.580
μ(Mo-Kα) [mm^{-1}]	2.845	2.68	2.46	2.29
F (000)	1524	1520	1516	1416
Reflns collected	28184	28220	28997	26061
Unique reflns	7240	7353	8275	6076
R_{int}	0.0779	0.0521	0.3682	0.0819
Param/restraints	379 / 0	379 / 0	379 / 0	379 / 0
GOF	1.004	1.045	0.814	1.029
R_1 [I > 2σ(I)]	0.0399	0.0405	0.0933	0.0478
wR_2 (all data)	0.0753	0.1078	0.1463	0.1203

Table S2. Parameters obtained by least-squares-fitting via the sum of two modified Debye functions at different DC field and 1.8 K for **2Dy**.

H/Oe	$\Delta\chi_1$/ cm^3 mol^{-1}	$\Delta\chi_2$/ cm^3 mol^{-1}	τ_1 /s	α_1	τ_2/s	α_2
0	18.17	0	8.87e-4	0.14	0	0
100	16.30	2.02	8.33e-4	0.19	0.08	0
200	11.02	7.50	7.06e-4	0.23	0.10	0.06
300	7.10	11.46	6.23e-4	0.29	0.14	0.12
400	4.10	14.00	4.83e-4	0.30	0.17	0.17
500	2.27	15.08	3.60e-4	0.25	0.19	0.19
1000	0	14.07	0	0	0.22	0.18

2000	0	8.91	0	0	0.16	0.17
3000	0	4.69	0	0	0.09	0.17

Table S3. Parameters of the biexponential fits of the Q-band relaxation measurements on **2Y**

Inversion Recovery				
Temperature / K	A_f	$T_{1,f}$ / ms	A_s	$T_{1,s}$ / ms
7	–1.3 ± 0.1	0.06 ± 0.01	–0.65 ± 0.04	0.9 ±0.1
Hahn-echo decay				
Temperature / K	A_f	$T_{m,f}$ / µs	A_s	$T_{m,s}$ / µs
7	1.0 ± 0.1	0.5 ± 0.1	0.36 ± 0.01	9 ± 2

Table S4. Calculated energies (in cm^{-1}) for the 16 energy levels of the $^6H_{15/2}$ ground multiplet of Dy^{III} in complexes **1Dy**, and projection of the total moment on quantization axis of every state.

	Energy /cm^{-1}	Projection of the total moment on quantization axis
1	0.000	80.8%|-15/2>+0%|-13/2>+0.6%|-11/2>+0.7%|-9/2>+0.3%|-7/2>+0.1%|-5/2>+0%|-3/2>+0.1%|-1/2> +17%|15/2 >+0%|13/2>+0.1%|11/2>+0.1%|9/2>+0.1%|7/2>+0%|5/2>+0%|3/2 >+0%|1/2>
2	4.99E-6	17%|-15/2 >+0%|-13/2>+0.1%|-11/2>+0.1%|-9/2>+0.1%|-7/2>+0%|-5/2>+0%|-3/2>+0%|-1/2>+ 80.8%|15/2>+0%|13/2>+0.6%|11/2>+0.7%|9/2>+0.3%|7/2>+0.1%|5/2>+0%|3/2>+0.1%|1/2>
3	84.497	0.1%|-15/2>+16%|-13/2>+5.4%|-11/2>+1.4%|-9/2>+1.1%|-7/2>+0.2%|-5/2>+0.1%|-3/2>+2.0%|-1/2> +0.2%|15/2 >+44.5%|13/2>+17.9%|11/2>+4.2%|9/2>+3.9%|7/2>+0.9%|5/2>+1.7%|3/2 >+0.5%|1/2>
4	84.497	0.2%|-15/2>+44.5%|-13/2>+17.9%|-11/2>+4.2%|-9/2>+3.9%|-7/2>+0.9%|-5/2>+1.7%|-3/2>+0.5%|-1/2> +0.1%|15/2>+16%|13/2>+5.4%|11/2>+1.4%|9/2>+1.1%|7/2>+0.2%|5/2>+0.1%|3/2>+2.0%|1/2>
5	122.856	0.1%|-15/2>+0.6%|-13/2>+1.1%|-11/2>+6.8%|-9/2>+0.7%|-7/2>+0.1%|-5/2>+5.5%|-3/2>+4.1%|-1/2> +0.5%|15/2 >+23%|13/2>+14%|11/2>+20.9%|9/2>+2.7%|7/2>+13.8%|5/2>+0.8%|3/2 >+5.1%|1/2>
6	122.856	0.5%|-15/2>+23%|-13/2>+14%|-11/2>+20.9%|-9/2>+2.7%|-7/2>+13.8%|-5/2>+0.8%|-3/2 >+5.1%|-1/2> +0.1%|15/2>+0.6%|13/2>+1.1%|11/2>+6.8%|9/2>+0.7%|7/2>+0.1%|5/2>+5.5%|3/2>+4.1%|1/2>
7	142.044	0.3%|-15/2>+4.2%|-13/2>+9.6%|-11/2>+9.8%|-9/2>+2.1%|-7/2>+4.4%|-5/2>+10.5%|-3/2>+8.1%|-1/2> +0.3%|15/2 >+1.6%|13/2>+14.8%|11/2>+0.7%|9/2>+18.8%|7/2>+3.5%|5/2>+8.9%|3/2 >+2.5%|1/2>
8	142.0447	0.3%|-15/2>+1.6%|-13/2>+14.8%|-11/2>+0.7%|-9/2>+18.8%|-7/2>+3.5%|-5/2>+8.9%|-3/2>+2.5%|-1/2> +0.3%|15/2>+4.2%|13/2>+9.6%|11/2>+9.8%|9/2>+2.1%|7/2>+4.4%|5/2>+10.5%|3/2>+8.1%|1/2>
9	172.307	0.1%|-15/2>+0.9%|-13/2>+3.4%|-11/2>+15.7%|-9/2>+1.4%|-7/2>+2.5%|-5/2>+10.4%|-3/2>+9.1%|-1/2> +0.1%|15/2 >+0.3%|13/2>+6.1%|11/2>+0.4%|9/2>+15.5%|7/2>+10.8%|5/2>+3.0%|3/2 >+20.1%|1/2>
10	172.307	0.1%|-15/2>+0.3%|-13/2>+6.1%|-11/2>+0.4%|-9/2>+15.5%|-7/2>+10.8%|-5/2>+3.0%|-3/2>+20.1%|-1/2> +0.1%|15/2>+0.9%|13/2>+3.4%|11/2>+15.7%|9/2>+1.4%|7/2>+2.5%|5/2>+10.4%|3/2>+9.1%|1/2>
11	221.7549	0.1%|-15/2>+3.5%|-13/2>+0.4%|-11/2>+5.6%|-9/2>+15.3%|-7/2>+17.3%|-5/2>+13.5%|-3/2>+0.2%|-1/2> +0.1%|15/2 >+3.5%|13/2>+2.6%|11/2>+4.2%|9/2>+14.4%|7/2>+15.2%|5/2>+3.9%|3/2 >+2.9%|1/2>
12	221.7549	0.1%|-15/2 >+3.5%|-13/2>+2.6%|-11/2>+4.2%|-9/2>+14.4%|-7/2>+15.2%|-5/2>+3.9%|-3/2 >+2.9%|-1/2>+ 0.1%|15/2>+3.5%|13/2>+0.4%|11/2>+5.6%|9/2>+15.3%|7/2>+17.3%|5/2>+13.5%|3/2>+0.2%|1/2>
13	259.231	0%|-15/2>+4.6%|-13/2>+22.9%|-11/2>+26.3%|-9/2>+15.3%|-7/2>+12.1%|-5/2>+9.7%|-3/2>+2.7%|-1/2> +0.0%|15/2>+0.1%|13/2>+0.1%|11/2>+0.1%|9/2>+0.7%|7/2>+1.8%|5/2>+1.5%|3/2 >+1.9%|1/2>
14	259.231	0.0%|-15/2 >+0.1%|-13/2>+0.1%|-11/2>+0.1%|-9/2>+0.7%|-7/2>+1.8%|-5/2>+1.5%|-3/2 >+1.9%|-1/2> +0.0%|15/2>+4.6%|13/2>+22.9%|11/2>+26.3%|9/2>+15.3%|7/2>+12.1%|5/2>+9.7%|3/2>+2.7%|1/2>

15	498.047	0.0%|-15/2>+0.1%|-13/2>+0.4%|-11/2>+1.5%|-9/2>+3.8%|-7/2>+7.3%|-5/2>+17.6%|-3/2>+15.3%|-1/2> +0.0%|15/2>+0.1%|13/2>+0.5%|11/2>+1.5%|9/2>+3.9%|7/2>+9.9%|5/2>+12.8%|3/2 >+25.3%|1/2>
16	498.047	0.0%|-15/2>+0.1%|-13/2>+0.5%|-11/2>+1.5%|-9/2>+3.9%|-7/2>+9.9%|-5/2>+12.8%|-3/2>+25.3%|-1/2> +0.0%|15/2>+0.1%|13/2>+0.4%|11/2>+1.5%|9/2>+3.8%|7/2>+7.3%|5/2>+17.6%|3/2>+15.3%|1/2>

Table S5. Calculated energies (in cm^{-1}) for the 13 energy levels of the $^7F_6$ ground multiplet of Tb^{III} in complexes **1Tb**, and projection of the total moment on quantization axis of every state.

	Energy /cm^{-1}	Projection of the total moment on quantization axis
1	0	45.3%|-6 >+2.7%|-4>+0.2%|-3>+1.3%|-2>+0.1%|-1>+0.8%|0>+ 45.3%|6 >+2.7%|4>+0.2%|3>+1.3%|2>+0.1%|1>
2	2.523	47.9%|-6 >+1.7%|-4>+0.1%|-3>+0.3%|-2> 47.9%|6 >+1.7%|4>+0.1%|3>+0.3%|2>
3	52.964	0.2%|-6 >+22.9%|-5>+1.5%|-4>+12.6%|-3>+1.3%|-2>+11%|-1>+0.9%|0>+ 0.2%|6 >+22.9%|5>+1.5%|4>+12.6%|3>+1.3%|2>+11%|1>
4	70.954	2.4%|-6 >+19%|-5>+8.8%|-4>+4.7%|-3>+8.8%|-2>+1.3%|-1>+9.9%|0>+ 2.4%|6 >+19%|5>+8.8%|4>+4.7%|3>+8.8%|2>+1.3%|1>
5	107.486	2.0%|-6 >+25.4%|-5>+7.9%|-4>+1.0%|-3>+8.1%|-2>+0.7%|-1>+9.8%|0>+ 2.0%|6 >+25.4%|5>+7.9%|4>+1.0%|3>+8.1%|2>+0.7%|1>
6	158.533	1.0%|-6 >+22.2%|-5>+12.6%|-4>+4.5%|-3>+2.2%|-2>+7.3%|-1>+0.5%|0>+ 1.0%|6 >+22.2%|5>+12.6%|4>+4.5%|3>+2.2%|2>+7.3%|1>
7	183.415	0.9%|-6 >+4.2%|-5>+28.7%|-4>+5.1%|-3>+2.8%|-2>+8.1%|-1>+0.4%|0>+ 0.9%|6 >+4.2%|5>+28.7%|4>+5.1%|3>+2.8%|2>+8.1%|1>
8	256.733	0.1%|-6 >+1.3%|-5>+22.4%|-4>+10.8%|-3>+15.1%|-2>+0.2%|-1>+0.2%|0>+ 0.1%|6 >+1.3%|5>+22.4%|4>+10.8%|3>+15.1%|2>+0.2%|1>
9	261.982	0.1%|-6 >+3.1%|-5>+4.5%|-4>+32.9%|-3>+7.8%|-2>+1.2%|-1>+0.9%|0>+ 0.1%|6 >+3.1%|5>+4.5%|4>+32.9%|3>+7.8%|2>+1.2%|1>
10	373.724	0.1%|-6 >+0.1%|-5>+3.3%|-4>+1.5%|-3>+12.5%|-2>+11.4%|-1>+42.3%|0>+ 0.1%|6 >+0.1%|5>+3.3%|4>+1.5%|3>+12.5%|2>+11.4%|1>
11	374.728	0.9%|-5>+0.4%|-4>+6.3%|-3>+5.2%|-2>+29.6%|-1>+15.3%|0>+ 0.9%|5>+0.4%|4>+6.3%|3>+5.2%|2>+29.6%|1>
12	412.974	0.6%|-5>+0.8%|-4>+18.1%|-3>+3.5%|-2>+26.4%|-1>+1.2%|0>+ 0.6%|5>+0.8%|4>+18.1%|3>+3.5%|2>+26.4%|1>
13	413.965	0.3%|-5>+4.8%|-4>+2.1%|-3>+31.1%|-2>+2.8%|-1>+17.7%|0>+ 0.3%|5>+4.8%|4>+2.1%|3>+31.1%|2>+2.8%|1>

Table S6. Elemental Analysis for compounds **1Ln** and **2Ln**.

Samples	C (%)		H (%)		N (%)	
	Found	Calc	Found	Calc	Found	Calc
1Dy	34.75	34.01	2.871	2.85	22.22	21.63
2Dy	38.95	39.7	3.211	3.20	20.1	21.36
1Tb	33.55	34.16	2.99	2.87	21.69	21.73
2Tb	39.29	39.88	3.169	3.22	20.25	21.46

1Gd	35.08	34.24	2.942	2.87	22.86	21.78
2Gd	39.55	39.97	3.248	3.22	21.06	21.51
1Y	38.50	37.57	3.314	3.15	24.70	23.90
2Y	43.35	43.8	3.571	3.53	22.93	23.57

Reference

[1] H.-J. Werner, P. J. Knowles, G. Knizia, F. R. Manby, and M. Schütz, WIREs Comput. Mol. Sci. **2,** 242 (2012).

[2] H.J. Werner, P.J. Knowles, G. Knizia, F.R. Manby, M. Schütz, P. Celani, W. Györffy, D. Kats, T. Korona, R. Lindh, A. Mitrushchenkov, G. Rauhut, K.R. Shamasundar, T.B. Adler, R.D. Amos, A. Bernhardsson, A. Berning, D.L. Cooper, M.J. O. Deegan, A.J. Dobbyn, F. Eckert, E. Goll, C. Hampel, A. Hesselmann, G. Hetzer, T. Hrenar, G. Jansen, C. Köppl, Y. Liu, A.W. Lloyd, R.A. Mata, A.J. May, S.J. McNicholas, W. Meyer, M.E. Mura, A. Nicklass, D.P. O'Neill, P. Palmieri, D. Peng, K. Pflüger, R. Pitzer, M. Reiher, T. Shiozaki, H. Stoll, A.J. Stone, R. Tarroni, T. Thorsteinsson, and M. Wang, *MOLPRO, version 2015.1, a package of ab initio programs* (2015, see www.molpro.net).

[3] C. Köppl and H.-J. Werner, J. Chem. Theory. Comput. **12,** 3122 (2016).

[4] P. P. Hallmen, C. Köppl, G. Rauhut, H. Stoll, and J. van Slageren, J. Chem. Phys. **147,** 164101 (2017).

[5] M. Dolg, H. Stoll, and H. Preuss, J. Chem. Phys. **90,** 1730 (1989).

[6] D. Andrae, U. Häußermann, M. Dolg, H. Stoll, and H. Preuß, Theoret. Chim. Acta **77,** 123 (1990).

[7] R. Gulde, P. Pollak, and F. Weigend, J. Chem. Theory. Comput. **8,** 4062 (2012).

[8] A. K. Wilson, D. E. Woon, K. A. Peterson, and T. H. Dunning, J. Chem. Phys. **110,** 7667 (1999).

[9] D. E. Woon and T. H. Dunning, J. Chem. Phys. **98,** 1358 (1993).

[10] D. E. Woon and T. H. Dunning, J. Chem. Phys. **100,** 2975 (1994).

[11] F. Weigend, Phys. Chem. Chem. Phys. **4,** 4285 (2002).

[12] G. Knizia, J. Chem. Theory. Comput. **9,** 4834 (2013).

[13] L. F. Chibotaru and L. Ungur, J. Chem. Phys. **137,** 64112 (2012).